

CHARACTERIZATION OF LAND USE \ LAND COVER CHANGES AND THEIR IMPACT ON LAND SURFACE TEMPERATURE USING REMOTE SENSING DATA IN EL-SHARQIA GOVERNORATE, EGYPT.

Sahar A. Shahin and Randa S. Makar

Soils and Water Use Department, Agricultural and Biological
Research Institute, National Research Centre, Egypt.

ABSTRACT

The changes in Land Use\ Land Cover (LULC) have significant consequences, such as increased land surface temperatures (LST). The present research investigated how the changes in LULC affected the LST in El-Sharqia Governorate, Egypt using remote sensing data from 2001 to 2022. The studied governorate is located to the east of the Nile Delta and considered one of Egypt's most productive agricultural areas. Nevertheless, the governorate underwent noticeable LULC changes whether through reclamation or urbanization due to the fast population growth. In this study, we used two Landsat images acquired on 2001 and 2022 to characterize the LULC changes in the studying area. Furthermore, the Normalized Difference Vegetation Index (NDVI) as indication of LULC was used to evaluate the impact of such changes on LST. NDVI data acquired from MODIS Vegetation Indices (MOD13Q1) was used as well as MODIS LST data (MOD11A2 and MOD11B3). Moreover, other factors such as air temperature affecting LST was also considered and their relation to LST was evaluated. The air temperature data was acquired from NASA's Prediction of Worldwide Energy Resource (POWER) project. The results revealed that five LULC classes were found in the study area including the vegetation, water, fallow soils, barren land and urban area. Vegetation was the major LULC during the study period. Most of the change in the study area was due land reclamation and urbanization affected by the fast population growth. There was a negative correlation between LST and NDVI and correlation was stronger in summer (July) than in winter (January). There was also a positive correlation between the monthly LST and the monthly air temperature of the same months. Nevertheless, the correlation was higher in winter than in summer. Therefore, it could be concluded that both urbanization and global warming effect increases LST but in winter the main factor affecting LST is air temperature while in summer the main factor is NDVI or the presence or absence of vegetation cover in the studied area.

Key Words: Land use/land cover change Land surface temperature Remote sensing Modis NDVI.

INTRODUCTION

Changes in land cover and use are currently identified as a primary cause of global change. Urbanization and population expansion is one of the key worldwide factors influencing LULC change (**Dumitrascu et al., 2023**). Furthermore, it is anticipated that urbanization will continue faster over the coming decades, especially in Africa (**UN, 2014**). The significance of the relationship between LULC, and land surface temperature (LST) fluctuate over the years (**Njoku and Tenenbaum, 2022**). Nevertheless, fast urbanization caused what is known as a "urban heat island" (UHI), where urban landscape will have comparatively higher temperatures than the surrounding rural areas (**Li et al., 2018**). Moreover, small towns as well as large cities started displaying heating problem and their monitoring could help to provide suitable adopting policies to overcome or minimize the problem (**Xie and Fan, 2021**). A study carried out by **Gyimah et al., (2023)** revealed that increasing urbanization by about 8.6% and declining vegetation cover by 2.5%, resulted an increase of 0.8 °C of the mean LST in 25 years in Accra, Ghana. In Egypt, a study in the Nile Delta revealed that urbanization of agricultural areas resulted in an increase in LST while the conversion from barren land to agriculture areas led to a decrease in LST (**Hereher, 2016**). Similarly, increasing built-up areas by 18.9% growth from 2001 to 2022 increased the LST in El-Sharqia Governorate, Egypt by 3.98% (**Fahmy et al., 2023**). Contrary, **Balas et al., (2023)** noticed an enhancement in LST caused by the increment in built-up area in a five-year period in Godhra region, India.

Furthermore, **Kawashima et al., (2000)** documented that surface temperature was strongly related to air temperature in the Kanto plain, Japan and its surrounding mountainous area. On the other hand, **Naserikia et al., (2023)** reported stronger relationships between LST and air temperature in natural areas (with mostly dense and scattered trees) compared to built up areas in Sydney metropolitan area, Australia. Moreover, greater LST seasonal variability was observed in the same area compared to air temperature and the spatial distribution for air temperature hot spots does not always overlap with LST.

Remote sensing data provided consistent and repetitive coverage of the earth surface conditions. Together with geographical information system are considered as the most effective and appropriate tool for evaluating the spatio-temporal LULC changes as well as the satellite-based land surface temperature (LST) and their relationship. In this aspect, various remote sensing indices have been

used to study the relationship between LULC and LST (**Njoku and Tenenbaum, 2022**). NDVI as a function of the LULC change was used by **Alexander (2020)** to monitor LST. The results showed that in the area where significant urbanization replaced arable lands and rangelands, the relationship between LST and NDVI showed a negative correlation and there was an increase in LST in rangelands and arable land, while it decreased in irrigated crops and arboriculture. Similar results were observed by **Yeneneh et al., (2022)** who found negative correlation between LST and NDVI. And the highest mean LST values were found on built-up areas and bare land, and the lowest values were recorded on forest land. **Waseem and Athar (2022)** also reported a negative correlation between LST and Green Vegetation Fraction (GVF) indicating that the decrease in vegetation cover resulted in an increase of LST. Overall, **El-Zeiny and Effat (2017)** recommended remote sensing and Geographic Information System (GIS) methodologies to evaluate the spatiotemporal changes in LULC induced by planned developmental projects or unregulated human activities as well as their correlation with LST. The current research delineated and evaluated the LULC changes El-Sharqia Governorate, Egypt over the course of 22 years by utilizing remote sensing data. Additionally, it assessed the influence of these changes on LST across the entire governorate.

MATERIALS AND METHODS

1. Study Area

El-Sharqia Governorate is located to the east of the Nile-Delta and bounded by longitudes 31° 19` and 32° 14` E and latitudes 30° 00` and 31° 11` N and covers an area of about 5331.6 km² (Figure 1). Surface elevation is around 10 m above the mean sea level (**Mohamed and Rashed, 2012**). The main landforms in the study area include flood plain, fluvio-lacustrine and aeolian deposits (**Ali, 2012**). The top soil in the western parts of the governorate near the Nile delta is dominated by Clay and silty soils, while the desert soils in the southern and eastern parts are dominated by sandy soils (**Rashed, 2016**).

El-Sharqia Governorate is characterized by a hot desert climate with high temperatures, low humidity all year round, and very little rain in winter (**Fahmy et al., 2023**). The highest monthly mean temperature is in July and August, while the lowest monthly mean temperature is in January (**Rashed, 2016**). The soil temperature regime of the studied area is defined as Thermic and the soil moisture regime as Torric (**Ali, 2012**). El-Sharqia Governorate represents about 10% of the total area of agricultural

land in Egypt and is considered one of its important agricultural governorates (Abdel-Rahman *et al.*, 2022). Vegetation varies from major field-crops such as maize and rice, to vegetables such as cucumber, potato and tomato. It is also a centre for the cotton and grain trade in Egypt (Rashed, 2016). The population in El-Sharqia Governorate is increasing and the governorate is continuously growing which is causing urbanization and increasing the demand for housing and other associated needs (Fahmy *et al.*, 2023).

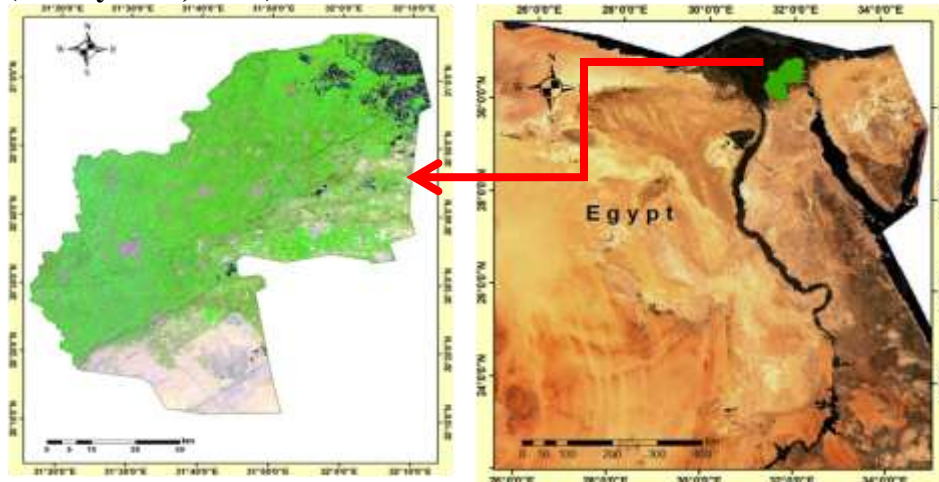


Figure 1. Location map of the studied area

2. Remote sensing data

2.1 Landsat data

Two satellite images (Path/Row: 17/39) acquired on 30-1-2001 from Landsat-7 and on 5-3-2022 from Landsat-8 have been utilized to determine the LULC changes in the study area. The images were freely available online via <https://earthexplorer.usgs.gov>. These top of atmosphere (TOA), atmospherically corrected surface reflectance data were geometrically corrected and projected into Universal Transverse Mercator (UTM) and World Geodetic System 1984 (WGS 84) with datum-zone 36 N. For each image the only blue (B), green (G), red (R), infrared (IR) and shortwave infrared (SWIR) bands of the images with a spatial resolution of 30 m were selected and used in this study. The images were imported and the selected bands were stacked into one multiband image for each date. Thereafter, each image was subsetted into the geographical extent

of the study area. The Landsat data were available in Geotiff format and processed using both the QGIS and ENVI software.

2.2. Landsat data processing

The supervised classification utilizing the maximum likelihood classification (MLC) was used to classify the different LULC classes. MLC is considered the most common supervised classification method used for analyzing satellite image data (**Ahmad and Quegan, 2012**). In the MLC, image pixels are assigned to the most likely class based on a comparison of the probability that it belongs to each of the signatures being considered (**Paul, 2014**). These signatures or training samples represent the different "spectral classes" and are used to estimate the parameters of a probability density function for each spectral class (**Bolstad and Lillesand, 1991**). The spectral separability between each two classes was estimated using the Jeffries-Matusita. In this evaluation, a threshold value of 1.8 is frequently used for accepting separation (**Yang et al., 2017**). Moreover, the overall accuracy of the classified image was examined. It is calculated as the percentage of the correctly classified validation pixels to the total number of pixels in the ground truth data (**Rwanga and Ndambuki, 2017**).

2.3. The Terra Moderate Resolution Imaging Spectroradiometer (MODIS) data

The Normalized Difference Vegetation Index (NDVI) of the MODIS Vegetation indices (MOD13Q1) Version 6.1 data was used in this study. These data are produced every 16 days at spatial resolution of 250 meter (m). From all the acquisitions within the 16 day period, the best available pixel with the highest value, low clouds and low view angle is selected to generate this product.

Moreover, the MODIS LST 8-Day (MOD11A2 Version 6.1) product was also used in this study. This product provides an average 8-day per-pixel daytime and nighttime LST at a 1 km spatial resolution. Additionally, the MODIS LST monthly product (MOD11B3 Version 6.1) which provides average monthly per pixel daytime and nighttime LST with a resolution of 5,600 m was used.

2.4. MODIS data Processing

The MODIS data were available in the Hierarchical Data Format (HDF) via the internet (<https://earthexplorer.usgs.gov>). The data were imported into the QGIS software, converted into Tiff format, subsetted to the geographical extent of the study area. For the MOD13Q1, only the NDVI layer was selected, while for

the MOD11A2 and MOD11B3, the LST values of day and night layers were selected and averaged into a single value per day. Additionally, MOD11B3 LST data was averaged for the whole study area to produce a single LST value per area per month.

2.5. Air Temperature data

The air temperature data used in this study were acquired from NASA's Prediction of Worldwide Energy Resource (POWER) project. These data was downloaded freely at <https://power.larc.nasa.gov/data-access-viewer>. The data had a grid resolution of 0.5 arc degree longitude by 0.5 arc degree latitude (Sparks, 2018). The POWER project draws its data from NASA sources such as World Climate Research Program, Global Energy and Water Cycle Experiment, Surface Radiation Budget Project and the Clouds and the Earth's Radiant Energy System projects at NASA LaRC, as well as the Global Modeling and Assimilation Office at the Goddard Space Flight Center (Akram *et al.*, 2022). The data representing the studied area included the monthly average temperature at 2 meters above the surface of the earth were collected.

2.6. Air temperature data analysis

The analysis of the air temperature data change from 2001 to 2022 included the application of the simple linear regression between time as independent and the temperature as the dependent. Its linear trend represented by the slop of the regression line of time verses temperature refers to the magnitude of rise or fall of the air temperature during the study period (Seltman, 2018). The mean annual temperature anomalies were also calculated. The anomalies represent the deviations from the mean values and therefore, facilitate accurate descriptions than the actual climatic parameters (Al-Muhyi *et al.*, 2016). Data air temperature data processing was applied using the Excel software.

RESULTS AND DISCUSSION

1. LULC classification and change detection

Based on literature, field work and knowledge of the studied area, five classes occupied the study area including the vegetation, water (fishponds and water), fallow soils (soils prepared for agriculture or to be used as fish farms), barren land (desert area) and urban area. Accordingly, the training samples were used to categorize the LU/LC classes of the study area and train MLC classifiers. After defining the training samples into the ENVI software, the separability between each two classes of the training sets was evaluated for the used six Landsat bands. According to Jeffries-Matusita measures, each two classes showed a

separability ranging between 1.6 and 2.0 for the image acquired on 2001, while it ranged between 1.5 and 2.0 for 2022 and most of the low values were acquired between the urban and fallow soils and the fallow soils and the fish farms due to their similar characteristics (**Gamba and Acqua, 2003**). Therefore, three indices were added to the used bands to increase the accuracy of the classification. These indices included the soil adjusted vegetation index (SAVI), modified normalized difference water index (NDWI) and the bare soil index (BSI).

The soil adjusted vegetation index (SAVI) was developed by **Huete (1988)** as follows:

$$SAVI = ((R_{IR} - R_R) / (R_{IR} + R_R + L)) \times (1 + L)$$

Where R refers to band reflectance, and the subscripts refer to a specific spectral band and L is the soil adjustment factor.

This index reduces the impact of soil brightness by including a soil adjustment factor L into the denominator of the normalized difference vegetation index (NDVI) equation. A value of 0.5 was recommended by **Qi et al., (1994)** for the L as it was found to minimize soil brightness variations and eliminate the need for additional calibration for different soils.

The Normalized Difference Water Index (NDWI) was developed by **McFeeters (1996)**. This index was developed to enhance delineation of open water features. The NDWI values range between -1 and 1, with the water or high humidity with a value of 1 and the dry areas or a lack of moisture with a value of -1. This index is defined as:

$$NDWI = (R_G - R_{NIR}) / (R_G + R_{NIR})$$

R refers to band reflectance, and the subscripts refer to a specific spectral band

Built-up areas and barren land are mostly misclassified as each other and this is partly because bare soil and urban features have relatively similar spectral characteristics (**Gamba and Acqua, 2003**). Bare soil indices generally include various bands with wavelengths ranging from visible to near-infrared and shortwave (**Nguyen et al., 2021**). The following equation defines the bare soil index (BSI) that was used in this study (**Chen et al., 2004**):

$$BSI = ((R_R + R_{SWIR1}) - (R_{NIR} + R_B)) / ((R_R + R_{SWIR1}) + (R_{NIR} + R_B))$$

R refers to band reflectance, and the subscripts refer to a specific spectral band

The inclusion of these three indices to the previously mentioned bands increased the Jeffries-Matusita measures between each two classes to reach more than 1.91 for both 2001 and 2022 images indicating that the classes are properly separated from each other.

Thereafter, the MLC classifier was used employing the training samples to categorize the different LULC classes of the study area on the two dates and the results are shown in Figure 2. The results showed that the overall accuracy was 87.5% and 93.7% for the images acquired in 2001 and 2022, respectively.

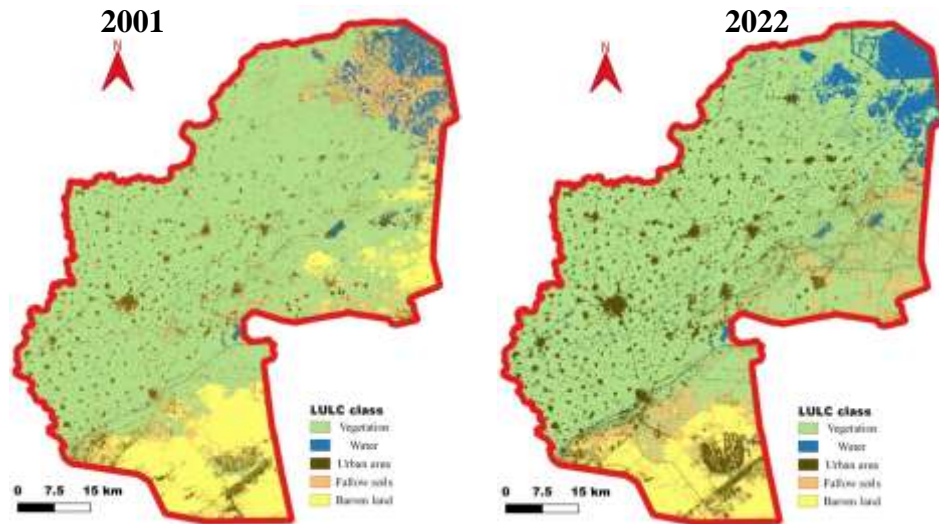


Figure 2. Land use/ land cover classification

The area covered by each LULC in 2001 and 2022 is shown in Table 1. Accordingly, most of the studied area was covered by vegetation, covering 65.5 % and 68.1 % of the studied area in 2001 and 2022, respectively. Most of the change in the study area was the decrease of the barren land (7.6 % of the studied area) and the increase of the urban area (4.2 % of the studied area).

Table 1. Acreage of the LULC classes of the studied area

LULC class	2001		2022		LULC change from 2001 to 2022	
	Km ²	%	Km ²	%	Km2	%
Vegetation	3493.1	65.5	3629.7	68.1	136.6	2.56
Water	187.4	3.5	319.7	6.0	132.3	2.48
Barren land	740.2	13.9	333.2	6.2	-407.0	-7.63
Fallow soils	487.3	9.1	400.8	7.5	-86.5	-1.62
Urban area	423.6	7.9	648.2	12.2	224.6	4.21
Total	5331.6	100.0	5331.6	100.0	0.0	0.00

2. Spatio-temporal changes of NDVI and LST

The NDVI of the MOD13Q1 V6.1 data acquired on 1-16 January (representing the winter season) and 12-27 July (representing the summer season) of years 2001, 2004, 2007,

2010, 2013, 2016, 2019, 2022 was collected and subsetted into the geographical extent of the study area and examples of which are shown in Figure 3. The LST day and night data of the MOD11A2 V6.1 was collected and subset into the geographical extent of the study area at the same period as NDVI data and average of the day and night values was calculated and used in this study. As every image represented 8-day only, the two images covering the same 16 days as the NDVI were collected and averaged to produce a 16 day value to evaluate the relationship between NDVI and LST as the same periods. Furthermore, the LST values were available in Kelvin and therefore, were subtracted by 273.15 to convert them to degrees Celsius and examples of which are shown in Figure 4.

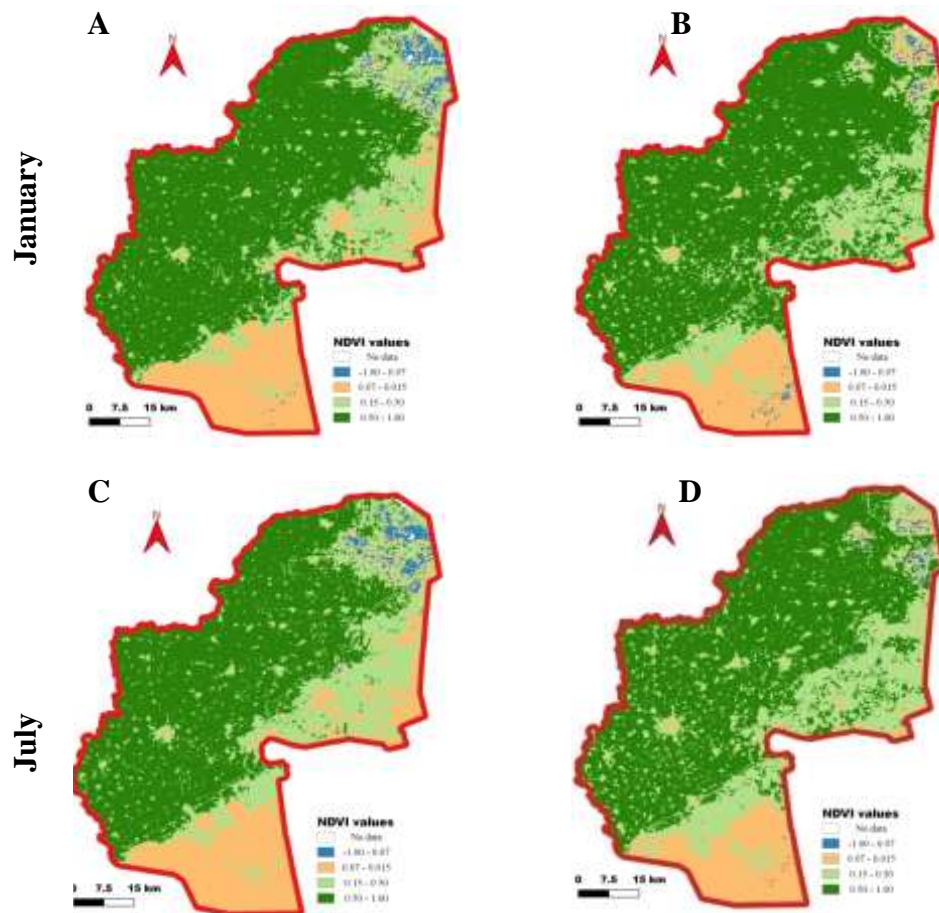


Figure 3. NDVI classifications in January (A) 2001 & (B) 2022 and July (C) 2001 & (D) 2022

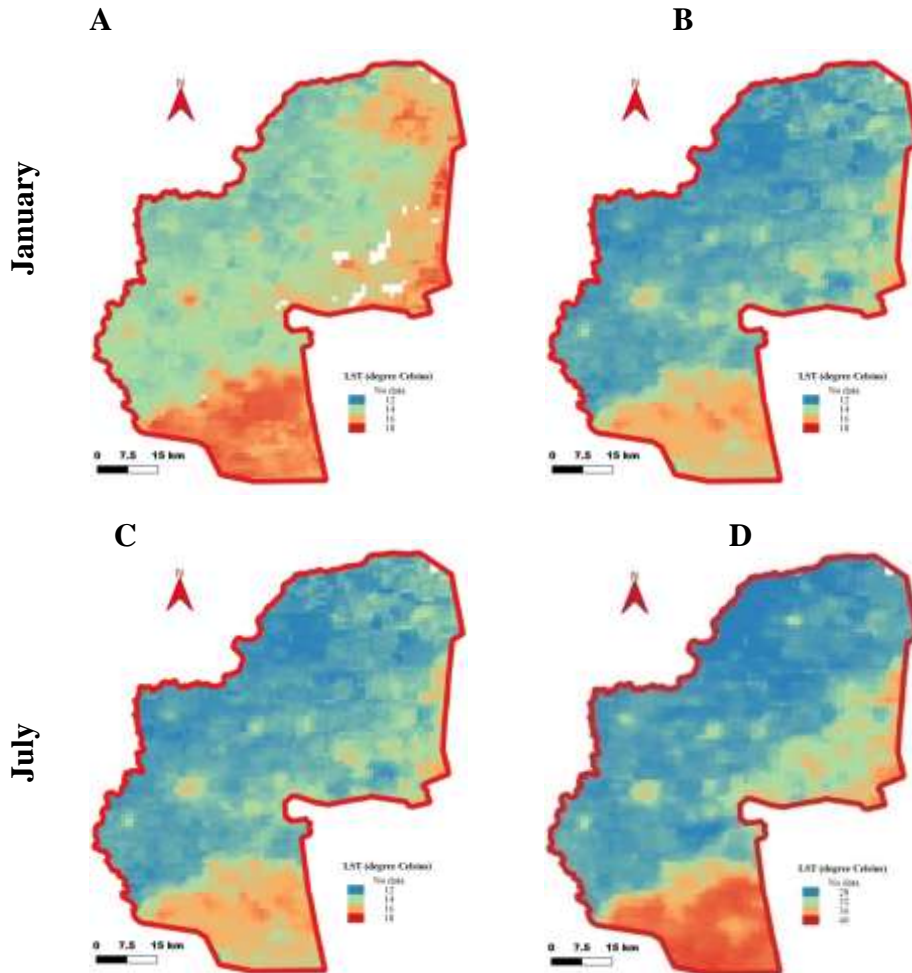


Figure 4. LST values in January (A) 2001 & (B) 2022 and July (C) 2001 & (D) 2022.

To evaluate the correlation between the LST and NDVI, 163 points were randomly selected covering all the observed LULC changes from 2001 to 2022 and the data of NDVI and LST at these locations were collected and analyzed using the Excel software. The correlation analyses between the two variables revealed that there was a negative correlation between NDVI and LST which is similar to the finding of **Njoku and Tenenbaum, (2022)**. In winter (January), there was a moderate negative correlation between LST and NDVI reaching r^2 of -0.50. Nevertheless, the two variables were strongly negatively

correlated in summer (July) reaching r^2 of -0.83. This implies that as the NDVI values increases, the LST decreases and such relationship is more profound in summer than in winter. Furthermore, higher NDVI value indicates a higher concentration of vegetation on the ground, while the negative values indicate non-green regions such as: barren, sea, river and built-up (Arval *et al.*, 2022) and therefore, NDVI is considered one of the significant classification methods widely used to classify LULC and their changes (Aburas *et al.*, 2015). To demonstrate the impact of each LULC on LST, representative points of each class which remained unchanged throughout the study period (2001-2022) were selected and the LST values were plotted verses time as shown in Figure 5. It was observed that in summer the barren land and fallow soils (with low NDVI values) had the highest temperature while in winter even so it followed the same trend, the impact of LULC is not as profound as seen in summer.

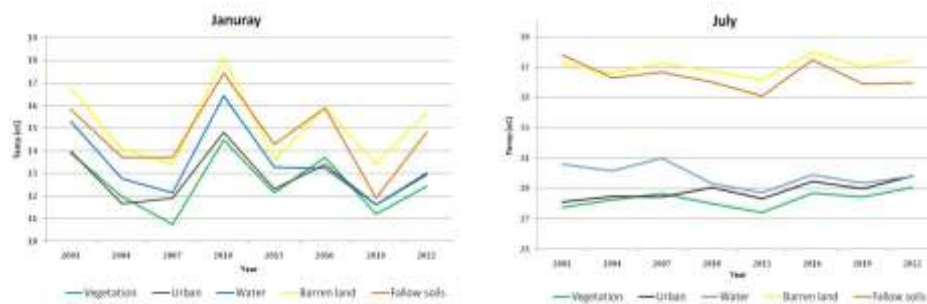


Figure 5. LST values of the different LULC class

To evaluate the impact of each LULC class on LST, the correlation between the LST and NDVI values of each LULC class was considered. The results revealed that in winter the correlation between LST and NDVI in the barren land and fallow soils was the highest reaching -0.75 and -0.62, respectively. The lowest correlation between the two variables was water and urban area (-0.17, 0.07, respectively). Furthermore, the correlation in the vegetated area had a value of -0.44 taking into account that this class covered most of the studied area. Except for the water and urban area, the data followed the same trend in summer and the correlation was -0.50, -0.54, -0.73, -0.78, -0.85, for, water, urban area, vegetation, fallow soils and barren land, respectively.

3. Temporal air temperature analyses and their relation with LST

The annual mean temperature acquired from 2001 to 2022 was plotted verses time and the linear trends are presented graphically in

figure 6. The lowest mean annual temperature was recorded in 2006 and was 22.90 °C while the highest was recorded in 2010 and reached 24.66 °C. The average annual temperature within the study period was 23.48 °C. There was an increased warming trend by a rate of 0.019 °C which is less than the increase in global average temperature reported by the IPCC, 2007 (Al-Muhyi *et al.*, 2016). Moreover, plotting the annual change anomalies of the mean temperature versus time (Figure 7) revealed that the slop was increasing from year to year verifying an overall increase in the temperature in the study area. It was also observed that change from year to year did not follow a specific pattern and there was a noticeable temperature increase in 2010.

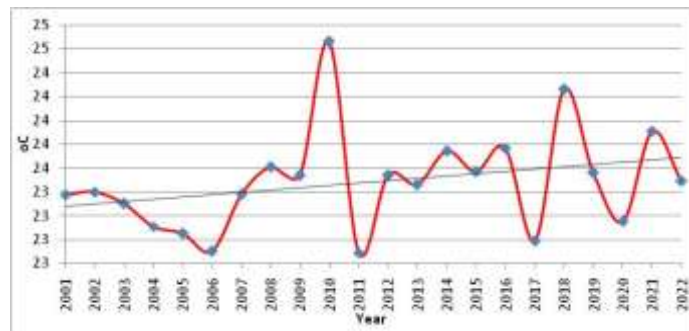


Figure 6. Annual mean temperature from 2001 to 2022

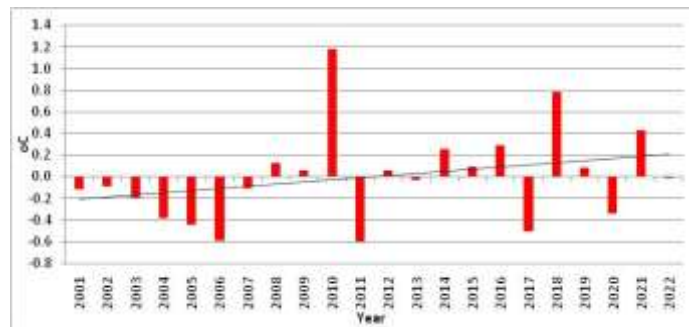


Figure 7. Anomalies of the annual mean temperature from 2001 to 2022.

To evaluate the correlation between LST and air temperature the monthly LST (MOD11B3) data was collected and subset into the geographical extent of the study area on January and July of the same studied years and average of the day and night values was calculated and averaged for the whole study area and the values were converted from Kelvin to degree Celsius.

Plotting the two variables versus time is shown in Figures 8 (January) and 9 (July). The correlation analysis between the two variables was evaluated and the results revealed that there was a positive correlation between LST and air temperature but it was higher in winter reaching 0.87 and only reached 0.65 in summer.

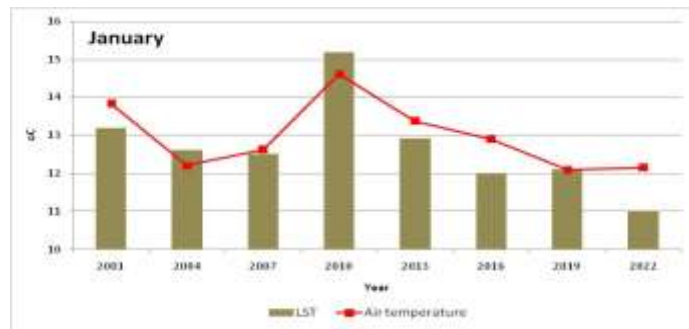


Figure 8.The monthly LST and air temperature values in January

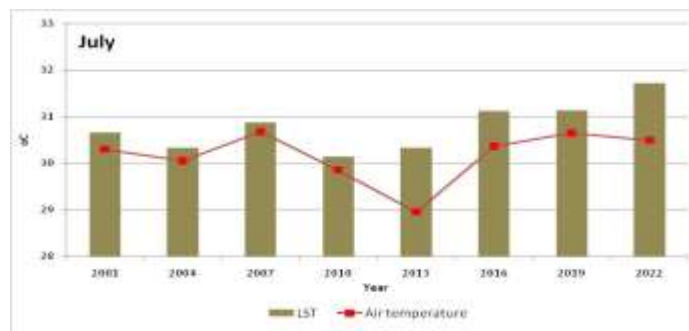


Figure 9.The monthly LST and air temperature values in July

CONCLUSION

In this study, two Landsat images acquired on 2001 and 2022 were used to characterize the LULC changes in El-Sharqia governorate. On the other hand, MODIS Vegetation Indices (MOD13Q1) data was also used as indication of LULC. Moreover, MODIS LST (MOD11A2) data was used to evaluate the relationship between LULC and LST and their changes throughout the study period from 2001 to 2022. The data was collected on 1-16 January and 12-27 July at a three years interval. Furthermore, to evaluate the impact of other factors such as air temperature on LST, the air temperature data acquired from NASA's POWER project at the same months was used. The

results revealed that, using the MLC classifiers, five classes were found in the study area including the vegetation, water, fallow soils, barren land and urban area and the overall classification accuracy was 87.5% and 93.7% for the images acquired in 2001 and 2022 respectively. Most of the studied area was occupied by vegetation covering more than 65 % of the studied area in 2001 and 2022. Furthermore, most of the change in the study area was in the form of urbanization and land reclamation. There was a negative correlation between LST and NDVI but the relationship was stronger in summer indicating that there were other factors affecting LST in the study area. Correlating the NDVI and LST in each LULC class, revealed that barren land and fallow soils had the highest correlation followed by vegetation and lastly were water and urban area. The low impact of urbanization could be because the studied governorate is mostly rural area and most of the urban areas are small towns and villages covering less than 15% of the studied governorate and most of it includes vegetation within the urban area.

There was a warming trend in air temperature observed in the study area from both the change in air temperature and the annual change anomalies from 2001 to 2022 and there was a noticeable temperature increase in 2010. Correlation analysis between the monthly LST and air temperature values of January and June of the studied years revealed that there was a positive correlation between LST and air temperature but it was higher in winter than in summer. Therefore, it could be concluded both air temperature and LULC change affects LST but in winter the main factor affecting LST was air temperature while in summer the main factor was NDVI or the presence of vegetation cover in the studied area.

REFERENCES

- Abdel-Rahman, M.A.E.; B. Engel ; M.S.M. Eid and H.M. Aboelsoud (2022).** A new index to assess soil sustainability based on temporal changes of soil measurements using geomatics – an example from El-Sharkia, Egypt. *ALL EARTH*, 34(1): 147-166.
- Aburas, M. ; Y.M. Ho ; M. Ramli and Z. Ashaari (2015).** Measuring Land Cover Change in Seremban, Malaysia Using NDVI Index. *Procedia Environ. Sci.*, 30: 238-243.
- Ahmad, A. and S. Quegan (2012).** Analysis of maximum likelihood classification technique on Landsat 5 TM satellite data of tropical land covers. In 2012 IEEE

International Conference on Control System, Computing and Engineering, pp. 280-285.

- Akram, H. ; D.F. Levia ; J.E. Herrick ; H. Lydiasari and N. Schütze (2022).** Water requirements for oil palm grown on marginal lands: A simulation approach. *Agricultural Water Management*. 260: 107292.
- Alexander, C. (2020).** Normalised difference spectral indices and urban land cover as indicators of land surface temperature (LST). *Int. J. Appl. Earth Obs Geoinformation*, 86: 102013.
- Ali, R.R. (2012).** The impact of land degradation on soil productivity in irrigated agriculture: A case study from El Sharkia Governorate, Egypt. *Australian J. Basic and Appl. Sci.*, 6(12): 453-463.
- Al-Muhyi A.H.A. ; A.L.A.J. Bashar and L.D.A. Kwyes (2016).** The study of climate change using statistical analysis case study temperature variation in Basra. *Int. J. Acad. Res.*, 2(5).
- Aryal, J. ; C. Sitaula and S. Aryal (2022).** NDVI threshold-based urban green space mapping from sentinel-2A at the local governmental area (LGA) level of Victoria, Australia. *Land*, 11:351.
- Balas, D.B. ; M.K. Tiwari ; M. Trivedi and G.R. Patel (2023).** Impact of land surface temperature (LST) and ground air temperature (Tair) on land use and land cover (LULC): An investigative study. *Int. J. Environ. and Climate Change*, 13(10): 3117-3130.
- Bolstad, P.V. and T.M. Lillesand (1991).** Rapid maximum likelihood classification. *Photogrammetric Engineering & Remote Sensing*, 57: 67-74.
- Chen, W.; L. Liu ; C. Zhang ; J. Wang ; J. Wang and Y. Pan (2004).** Monitoring the seasonal bare soil areas in Beijing using multi-temporal TM images. *IGARSS IEEE International Geoscience and Remote Sensing Symposium*, Anchorage, AK, 5: 3379-3382.
- Dumitrascu, M.; Y. Himiyama ; M. Gabrovec ; M. Kopecká ; L. Kupková and I. Bicik (2023).** Land Use and Land Cover Changes in a Global Environmental Change Context—The Contribution of Geography. In: Bański, J., Meadows, M. (eds) *Research Directions, Challenges and*

Achievements of Modern Geography. Advances in Geographical and Environmental Sciences, Springer, Singapore.

- El-Zeiny, A. and H.A. Effat (2017).** Environmental monitoring of spatiotemporal change in land use/land cover and its impact on land surface temperature in El-Fayoum governorate, Egypt. *Remote Sensing Applications: Society and Environ.*, 8: 266-277.
- Fahmy, A.H.; M.A. Abdelfatah and G. El-Fiky (2023).** Investigating land use land cover changes and their effects on land surface temperature and urban heat islands in Sharqiyah Governorate, Egypt. *The Egyptian J. Remote Sensing and Space Sci.*, 26: 293-306.
- Gamba, P. andAcqua, F.D. (2003).** Increased accuracy multiband urban classification using a neuro-fuzzy classifier. *Int. J. Remote Sens.*, 24: 827–834.
- Gyimah, R.R. ; C. kwang ; R.A. Antwi ; E.M. Attua ; A.B. Owusu and E.K. Doe (2023).** Trading greens for heated surfaces: Land surface temperature and perceived health risk in Greater Accra Metropolitan Area, Ghana. *The Egyptian J. Remote Sensing and Space Sci.*, 26: 861–880.
- Hereher, M. (2016).** Effect of land use/cover change on land surface temperatures - The Nile Delta, Egypt. *J. African Earth Sci.*, 126. <https://doi.org/10.1016/j.jafrearsci.2016.11.027>.
- Huete, A.R. (1988).** A soil-adjusted vegetation index (SAVI). *Remote Sens. Environ.*, 25: 295-309.
- Kawashima, S. ; T. Ishida ; M. Minomura and T. Miwa (2000).** Relations between surface temperature and air temperature on a local scale during winter nights. *J. Appl. Meteorol.*, 39:1570-1779.
- Li, J.; X. Zheng ; C. Zhang and Y. Chen (2018).** Impact of land-use and land-cover change on meteorology in the Beijing–Tianjin–Hebei region from 1990 to 2010. *Sustainability*, 10:176.
- McFeeters, S. K. (1996).** The use of the Normalized Difference Water Index (NDWI) in the delineation of open water features. *Int. J. Remote Sensing*, 17(7): 1425-1432.

- Mohamed, Y.A. and M. Rashad (2012).** Water resources management: Case study of Sharkia Governorate, Egypt. *Appl. Water Sci.*, 2: 95-99.
- Naserikia, M. ; M.A. Hart ; N. Nazarian ; B. Bechtel ; M. Lipson, and K.A. Nice (2023).** Land surface and air temperature dynamics: The role of urban form and seasonality. *Sci. of the Total Environ.*, 905: 167306.
- Nguyen, C.T. ; A. Chidthaisong ; P. Kieu Diem and L.Z. Huo (2021).** A Modified bare soil index to identify bare land features during agricultural fallow-period in Southeast Asia using landsat 8. *Land*, 10: 231.
- Njoku, E.A. and D.E. Tenenbaum (2022).** Quantitative assessment of the relationship between land use/land cover (LULC), topographic elevation and land surface temperature (LST) in Ilorin, Nigeria. *Remote Sensing Applications. Society and Environ.*, 27: 100780.
- Qi, J. ; A. Chehbouni ; A.R. Huete ; Y.H. Kerr and S.A. Sorooshian (1994).** Modified soil adjusted vegetation index. *Remote Sens. Environ*, 48: 119-126.
- Paul, S.S. (2014).** Analysis of land use and land cover change in Kiskatinaw River Watershed: A remote sensing, gis& modeling approach. Master Thesis, Natural Resources and Environmental Studies (Environmental Science), University of Northern British Columbia, USA.
- Rashed, H.S.A. (2016).** Determination of Soil Productivity Potentials: A Case Study in El-Sharkia Governorate of Egypt. *Egypt. J. Soil Sci.*, 56(4): 639-665.
- Rwanga, S.S. and J.M. Ndambuki (2017).** Accuracy assessment of land use/land cover classification using remote sensing and GIS. *Int. J. Geo Sci.*, 8: 611-622.
- Seltman, H. J. (2018).** Experimental Design and Analysis. <https://www.stat.cmu.edu/~hseltman/309/Book/Book.pdf> .
- Sparks, A.H. (2018).** NASA POWER: A Nasa power global meteorology, surface solar energy and climatology data client for R. J. Open Source Softw., 3: 1035.
- UN (2014).** World Urbanization Prospects: The 2014 Revision, Highlights. United Nations Department of Economic and Social Affairs, UN, New York.

- Waseem, A. and H. Athar (2022).** LST variability and population growth in district of Rawalpindi, Pakistan during 1993–2018: A regional climate model based bias correction approach for LST. The Egyptian J. Remote Sensing and Space Sci., 25: 975-985.
- Xie, F. and H. Fan (2021).** Deriving drought indices from MODIS vegetation indices (NDVI/EVI) and Land Surface Temperature (LST): Is data reconstruction necessary?. Int. J. Appl. Earth Observations and Geoinformation, 101: 102352.
- Yang, C. ; G. Wu ; K. Ding ; T. Shi ; Q. Li and J. Wang (2017).** Improving Land Use/Land Cover Classification by Integrating Pixel Unmixing and Decision Tree Methods. Remote Sensing, 9: 1222.
- Yeneneh, N. ; E. Elias and G.L. Feyisa (2022).** Detection of land use/land cover and land surface temperature change in the Suha Watershed, North-Western highlands of Ethiopia. Environ. Challenges, 7: 100523.

توصيف التغير في استخدامات الأراضي و تأثيرها علي درجة حرارة سطح الأرض باستخدام
بيانات الاستشعار عن بعد في محافظة الشرقية، مصر.

سحر عبدالله سليم السيد شاهين ، رائده شفيق جورجي

قسم الأراضي و استغلال المياه، معهد البحوث الزراعية و البيولوجية، المركز القومي للبحوث

التغيرات في استخدامات الأراضي و الغطاء الأرضي لها عواقب مهمة مثل ارتفاع درجات حرارة سطح الأرض. يهدف هذا البحث الى دراسة كيفية تأثير التغيرات في استخدامات الأراضي و الغطاء الأرضي على درجة حرارة سطح الأرض في محافظة الشرقية، مصر باستخدام بيانات الاستشعار عن بعد. تقع منطقة الدراسة شرق دلتا النيل و تعتبر من أكثر المناطق الزراعية انتاجية في مصر. و مع ذلك فقد شهدت المحافظة تغيرات ملحوظة في الغطاء الأرضي سواء من خلال استصلاح الأراضي الجرداء او التوسع العمراني بسبب النمو السكاني السريع. في هذه الدراسة تم استخدام صورتين من صور لاندسات لعامي 2001, 2022 لتوصيف التغيرات في استخدامات الأراضي و الغطاء النباتي. علاوة على ذلك، استُخدم دليل NDVI كمؤشر على هذه التغيرات ولتقييم تأثير هذه التغيرات على درجة حرارة سطح الأرض. بالإضافة لذلك تم دراسة عوامل أخرى مثل درجة حرارة الهواء و تقييم علاقتها بدرجة حرارة سطح الأرض. كشفت النتائج عن وجود خمس انواع من استخدامات الأراضي

فى منطقة الدراسة وهى الاراضى الزراعية ، المياه ، الاراضى القاحلة ، الاراضى الغير منزرعة و المناطق السكنية. و كانت معظم التغيرات فى منطقة الدراسة تتمثل فى استصلاح الاراضى وزيادة المناطق الحضرية نتيجة للزيادة السريعة فى النمو السكانى. كان هناك ارتباط سلبى بين درجة حرارة الارض و دليل NDVI و كان الارتباط أقوى فى الصيف (يوليو) عنه فى الشتاء (يناير). كان هناك أيضًا ارتباط إيجابى بين درجة حرارة سطح الارض ودرجة حرارة الهواء لنفس الأشهر ولكن كان الارتباط أعلى فى الشتاء عنه فى الصيف. ولذلك، يمكن استنتاج أن كلا من زيادة المناطق الحضرية وارتفاع درجة حرارة الهواء يعمل على زيادة درجة حرارة سطح الارض ولكن العامل الرئيسى الذى يؤثر على درجة حرارة سطح الارض فى الشتاء هو درجة حرارة الهواء، بينما العامل الرئيسى فى الصيف هو دليل NDVI او وجود/غياب الغطاء النباتى.